

Tomasch-effect study of the Fermi surface of lead*

T. W. Haywood,[†] J. D. Byrd,[‡] and E. N. Mitchell

Department of Physics and Astronomy, University of North Carolina, Chapel Hill, North Carolina 27514

(Received 11 December 1974)

An improved technique for the resolution of the periods of multiple-frequency Tomasch oscillations is presented. The technique has allowed the observation of Tomasch periods in epitaxial Pb films which differ from previous investigations in both value and number of frequencies present for a given tunneling direction, and has resolved second-harmonic structure in some oscillations. The periods obtained are used to map the phonon renormalization $Z(0)$ over the Fermi surface, and imply that in superconducting Pb the effective band mass is approximately equal to the free-electron mass.

I. INTRODUCTION

This paper reports an investigation of the relation between the period of Tomasch oscillation in superconducting, single-crystal Pb films and the Fermi surface of Pb at specific sites on the Fermi surface. The Tomasch effect is an oscillation in the density of electronic states of a superconductor with a period inversely proportional to the Fermi velocity, and is directly observable in the current-voltage characteristics of a tunnel junction fabricated with the superconductor. Since its initial discovery in 1965,¹ the effect has promised to be a valuable tool in the investigation of the Fermi surface. However, the general occurrence of more than one oscillation frequency coupled with a restriction of the data to only two or three periods of the oscillations has deterred the use of the effect as an investigative tool.

A previous investigation by Lykken *et al.*² of multiple-frequency Tomasch data in Pb found a considerable difference between values of the renormalized Fermi velocity $v_F/Z(0)$ obtained from Tomasch oscillations and those calculated with Anderson and Gold's four-orthogonal-plane-wave (4-OPW) model of the Fermi surface of Pb.³ In the theoretical calculation of that study² a constant value for the phonon renormalization of the effective mass, $Z(0)$, equal to its polycrystalline value of 2.33 (Ref. 4) was used. Calculations of mass enhancement $Z(0)$ by Anderson and Gold³ showed considerable variation among various orbits on the Fermi surface, implying anisotropy in $Z(0)$, but not enough anisotropy to account for the discrepancy found by Lykken *et al.*²

In this paper a new analysis technique for Tomasch oscillation periods and an extension of the tunneling investigation to several new orientations of Pb films has allowed a possible explanation of the previous discrepancies.

II. EXPERIMENTAL METHODS

Tunneling measurements were made on Pb-PbO-Pb-Ag tunnel junctions. The Pb-Ag films were deposited epitaxially on single-crystal KBr substrates by techniques established in this laboratory⁵ such that 700–1300-Å Ag films backed the 2.5–3.5- μm Pb films. The crystal orientation of these films were those of the KBr substrates and were subsequently checked using Laue back-reflection x-ray patterns which also monitored the quality of the epitaxy. The Pb films were oxidized by various means⁵ to form the tunneling barriers and polycrystal Pb films 3000–5000-Å thick then deposited to complete the fabrication of the tunnel junctions. For all junctions in the study the ratios of dI/dV at bias voltages less than that of the conductance peak to that at bias voltages greater than that of the conductance peak were less than 5×10^{-3} . Principal data for the study consisted of dV/dI measurements over the bias voltage range 2.9–5.2 mV.

III. THEORY OF TUNNELING WITH TOMASCH OSCILLATIONS

A. Tunneling current

The expression for the tunneling current at 0°K is given by

$$I = \sum_{p_{\perp}} C_{p_{\perp}} \int_{\Delta_{01}}^{V-\Delta_{02}} \rho_1(\omega)_{p_{\perp}} \rho_2(V-\omega)_{p_{\perp}} d\omega + \sum_{p_{\perp}} C_{p_{\perp}} \int_{\Delta_{01}}^{V-\Delta_{02}} \rho_1(\omega)_{p_{\perp}} \delta\rho_2(V-\omega)_{p_{\perp}} d\omega,$$

where $C_{p_{\perp}}$ limits the tunneling current to momentum states perpendicular to the tunneling barrier, V is the bias voltage across the tunnel junction, Δ_{01} (Δ_{02}) is the superconducting BCS energy gap of metal 1 (metal 2), $\rho_1(\omega)$ [$\rho_2(\omega)$] is the quasi-particle density of states of metal 1 (metal 2),

and $\delta\rho_2(\omega)$ is the contribution of the Tomasch oscillations to the density of states of metal 2. Here metal 1 is the polycrystal Pb film and metal 2 is the single-crystal Pb film. The quasiparticle density of states is given by

$$\rho(\omega)_{p_\perp} = \text{Re}\{\omega/[\omega^2 - \Delta^2(\omega)_{p_\perp}]^{1/2}\},$$

where $\Delta(\omega)_{p_\perp}$ is the complex energy gap at a point on the Fermi surface sampled by electrons with momentum p_\perp . The Tomasch term over the energy region of interest in this study can be expressed as

$$\delta\rho(\omega)_{p_\perp} = A(\omega) \cos[(2d/\hbar v_{g\perp}) \text{Re}\Omega(\omega)_{p_\perp}] + O(4d/\hbar v_{g\perp}),$$

where d is the thickness of the film. The amplitude $A(\omega)$ decreases rapidly with increasing energy. The term $\Omega(\omega)_{p_\perp}$ is given by

$$\Omega(\omega)_{p_\perp} = Z(\omega)_{p_\perp} [\omega^2 - \Delta^2(\omega)_{p_\perp}]^{1/2},$$

where $Z(\omega)_{p_\perp}$ is the complex phonon renormalization at the sampled point on the Fermi surface. $Z(\omega)$ modifies the effective mass of the electron such that⁶

$$\frac{m^*}{m_c} = Z(0) = 1 + \int_0^\infty d\omega \frac{2\alpha^2(\omega)}{\omega} F(\omega),$$

where m^* is the total effective electron mass, m_c is the Coulomb and band-dressed effective mass, $\alpha(\omega)$ is the electron-phonon coupling constant, and $F(\omega)$ is the phonon density of states. The term $v_{g\perp}$ is given by $\hat{n} \cdot \nabla_p \epsilon|_{p=p_\perp}$, where \hat{n} is the normal to the film surface. Terms of order $4d/\hbar v_{g\perp}$ allow for harmonic contributions as in the Wolfram theory of the Tomasch effect.⁷

B. Selection rules

Whether or not $v_{g\perp}$ is the Fermi velocity depends on which tunneling selection rule is applicable. The traditional tunneling selection rule is that only those electrons which have group velocity normal to the tunneling barrier contribute to the current. In this instance the group momentum $p_\perp = mv_{g\perp}$ would be normal to the Fermi surface and the film surface so that $v_{g\perp}$ would be the Fermi velocity of those electrons which contribute to the tunneling current. The selection process proposed by Dowman *et al.*⁸ requires that tunneling electrons have this phase momentum ($p_\perp = \hbar k_\perp$) perpendicular to the tunneling surface. In this instance $v_{g\perp}$ need not be normal to the Fermi surface and therefore need not be the Fermi velocity. This latter case would generally require that $v_{g\perp}$ measured by the Tomasch effect be smaller than the Fermi velocity at the corresponding point on the Fermi surface.

To determine which selection rule applies to Pb,

it is convenient to look at the prediction of the two methods for the number of energy gaps observed in specific tunneling directions. Haywood and Mitchell⁹ have shown that tunneling into epitaxial Pb films shows definite anisotropy with only a 5° change in tunneling direction. Thus a specific tunneling configuration very nearly measures a single specific direction in the crystal. Tunneling in a [111] direction in single-crystal Pb samples five separate points on the Fermi surface according to the group-velocity selection rule, but a single point according to the phase-velocity selection rule. Similarly, tunneling in the [100] direction samples three points with group-velocity selection and one point with phase-velocity selection. Dowman *et al.*⁸ point out that it may also be possible to tunnel by means of evanescent states in the insulator to add some undetermined sampling points in the phase-velocity selection process.

Bennett¹⁰ has calculated the energy gaps measured in these directions on the basis of the group-velocity selection rule. He predicts three distinct gaps in [100] tunneling and two distinct gaps in [111]. If direct k -vector coupling through the imaginary- k states of the insulator band gap is not considered, the phase-velocity selection limits the observable number of gaps to one in each of these two directions as only one point on the Fermi surface is sampled. Blackford¹¹ has observed two gaps tunneling in each direction into bulk, single-crystal Pb. Lykken *et al.*² have observed three gaps in [100] tunneling and two in [111] tunneling into epitaxial Pb films. This paper interprets the results of Lykken *et al.* as supporting the group-velocity selection rule for governing the tunneling process in the epitaxial Pb films of this study.

IV. ANALYSIS OF THE DATA

A. Period analysis

The analysis assumed the dV/dI data to be of the form

$$F(V) = \sum_j A_j(V) \cos[k_j \Omega_0(V) + \phi_j] + B(V),$$

where V is the bias voltage, $A_j(V)$ is an amplitude decay term for the j th component, ϕ_j is an undetermined constant phase factor on the j th component, $B(V)$ is the dV/dI background without Tomasch oscillations,

$$k_j = 2d/[\hbar v_{g\perp}/Z(0)]_j,$$

and

$$\Omega_0(V) = \frac{\text{Re}Z(V - \Delta_0)}{Z(0)} \{(V - \Delta_0)^2 - [\text{Re}\Delta_3(V - \Delta_0)]^2\}^{1/2}.$$

Here Δ_0 is the BCS energy gap of the polycrystal

film and $\Delta_s(V - \Delta_0)$ is the energy-dependent gap of the single-crystal film. The anisotropy in the renormalization Z is assumed to be independent of energy so that variations in Z with crystal orientation are contained in the renormalized velocity $v_{g\perp}/Z(0)$. The phase shift due to anisotropy in Δ_s has been assumed constant over the range of the data and is represented by ϕ_j . As indicated, the imaginary parts of Z and Δ_s are neglected as no significant differences were found by using the full complex values in representative test examples. It was further assumed that the amplitude terms of the several oscillations differed by constant factors so that the data could be represented by

$$F(V) = A(V) \sum_j a_j \cos[k_j \Omega_0(V) + \phi_j] + B(V),$$

where the a_j 's are constants.

The experimental data corresponding to $F(V)$ were points on the dV/dI curve 0.02-meV apart over the voltage range where Tomasch oscillations were discernable, and were measured in terms of the resistance of the junction at the corresponding point on the dV/dI plot. It was observed that the backgrounds $B(V)$ to the tunneling curves for all of the orientations studied were qualitatively similar. Therefore a single background shape was fitted to all the data.

The background was assumed to be of the form $B(V) = aB'(V) + R_0$, where a and R_0 varied from junction to junction. A careful measure of one hand-drawn background obtained a basic value of $B'(V)$ which was then used to fit a background to all data using two points of each data set to determine its respective a and R_0 . Fig. 1 shows a typical data set with the fitted background. The background so obtained was subtracted from the initial data to obtain points representing the Tomasch oscillations alone. This adjusted data was then

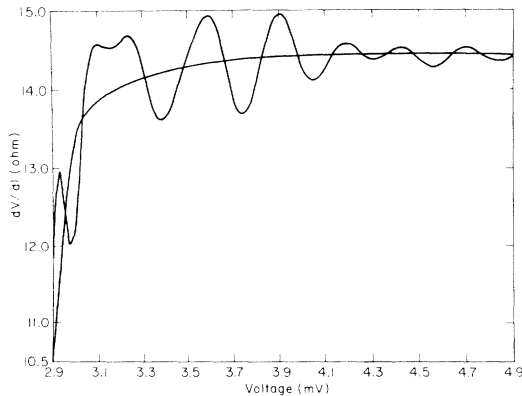


FIG. 1. Representative Tomasch oscillation data showing fitted background.

approximately compensated for the decay term $A(V)$ by dividing it by an envelope term of the form $A(V) = (V - \Delta_0) \text{Re}\Delta_s / \text{Re}Z\Omega_0^3$ derived from the McMillan-Anderson¹² theory of the Tomasch effect. The data of Fig. 1 thus compensated is shown in Fig. 2 and is of the general form

$$F_c(V) \approx \sum_j a_j \cos(k_j \Omega_0 + \phi_j).$$

A Fourier transform was then obtained directly in terms of $k' = 2d/\hbar [v_{g\perp}/Z(0)]'$ by numerically calculating

$$f(k') = \left(\int_{V_i}^{V_f} F_c(V) \sin[k' \Omega_0(V)] \frac{d\Omega_0}{dV} dV \right)^2 + \left(\int_{V_i}^{V_f} F_c(V) \cos[k' \Omega_0(V)] \frac{d\Omega_0}{dV} dV \right)^2,$$

where V_i and V_f are the bias voltages corresponding to the first and last data points, respectively, and $d\Omega_0/dV$ considers explicitly the voltage dependence of both $\text{Re}Z(V)$ and $\text{Re}\Delta_s(V)$ to achieve maximum resolution in the Fourier spectrum. The results of this operation were of the form shown in Fig. 3. Tests of the program using arbitrary a_j , $[v_{g\perp}/Z(0)]_j$, and ϕ_j showed the program to be insensitive to a_j and ϕ_j and returned the exact $[v_{g\perp}/Z(0)]_j$ designated in the test function. Variations in the background fit sometimes caused long-wavelength contributions corresponding to values of $v_{g\perp}/Z(0)$ greater than 10^8 cm/sec in the form of broad, low-level peaks in the plot of the transform. For this reason all such peaks were discarded when determining the actual $v_{g\perp}/Z(0)$ present in the oscillations. The results of this study are shown in Table I along with the previous results of Lykken *et al.*,² who used a different analysis technique. Noise peaks were randomly gen-

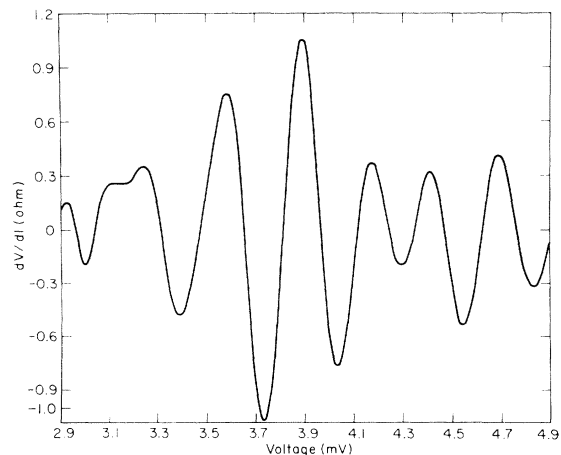


FIG. 2. Data of Fig. 1 after subtracting the background and compensating for amplitude decay.

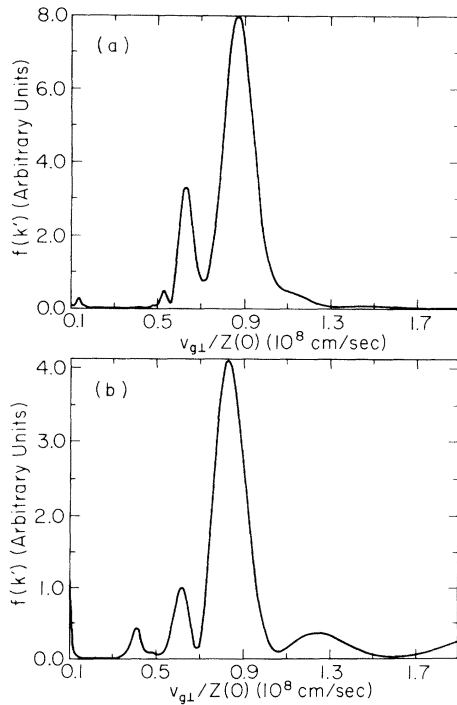


FIG. 3. Representative velocity spectra of the Fourier analysis: top, a typical spectrum for [311] tunneling; bottom, spectrum from [311] sample showing second harmonic (peak at $v_{g\perp}/Z(0) = 0.40$).

erated in data acquisition. Peak levels below 10% of the major peaks were discarded as noise unless they were present in several samples. The peak at $v_{g\perp}/Z(0) = 0.55$ in Fig. 3(a) is an example of this.

During the course of the study two films were observed to exhibit larger than usual oscillations. The films could not be distinguished in any other respect from others of the same orientation. The large oscillations were credited to some improvement in the electron mean free path of the film

TABLE I. Experimental $v_{g\perp}/Z(0)$ in 10^8 cm/sec.

Tunneling direction	$v_{g\perp}/Z(0)$		
[110]	0.54 ± 0.03	0.63 ± 0.03 (0.60 ± 0.05) ^a	0.85 ± 0.02 (0.94 ± 0.05) ^a
[111]		0.65 (0.60 ± 0.10) ^a	0.94 (1.17 ± 0.10) ^a
[211]		0.67	0.94
[311]		0.64	0.86
[100]		0.64 (0.69 ± 0.10) ^a	0.86 (1.05 ± 0.05) ^a
[210]	0.52	0.65	0.80

^a From Lykken *et al.*, Ref. 2.

which was incidental to an improvement in film quality. The transform of the oscillations of both films showed a peak corresponding to the second harmonic of the longest wavelength oscillation. The transform of one of these is shown in Fig. 3 and compared with the transform of another film of the same orientation not showing the harmonic contribution. Of the various theories of the Tomasch effect, only that of Wolfram⁷ allows the possibility of harmonic terms.

B. Application to the Fermi surface

If one compares the average value of $v_{g\perp}/Z(0)$ for the [100], [110], and [111] directions in this experiment to the average value of the Fermi velocity calculated² at the expected tunneling sites using Anderson and Gold's model of the Fermi surface, one finds an implied average value of 1.58 for $Z(0)$. McMillan and Rowell⁴ have calculated a value of 2.33 for $Z(0)$ using phonon spectra derived from tunneling data on polycrystal Pb. Such a discrepancy is not allowed by the errors in any of the measurements reported here. The relevant question that must be addressed is why phonon spectra imply one value for $Z(0)$ and Tomasch oscillations for another. It is the main purpose of the rest of this paper to at least shed some light on this question.

To isolate the source of the discrepancy the Fermi surface was represented by the effective-mass model

$$\epsilon(k_F) = \hbar^2 k_F^2 / 2m_0(m_b/m_0),$$

where m_0 is the free-electron mass and the band mass m_b contains all information on the curvature of the Fermi surface. The various k_F were assumed to be those measured by Anderson and Gold.³ The velocity selection is determined by

$$v_{g\perp} = \hat{n} \cdot \bar{\nabla}_p \epsilon|_{p=p_L} = \hbar k_{\perp} / m_0(m_b/m_0),$$

where k_{\perp} is that component of k perpendicular to the tunneling surface at the tunneling site on the Fermi surface. A map of the Fermi surface of Pb showing the tunneling sites and k_{\perp} vectors used in this study is given in Fig. 4. Calculations at each of the tunneling sites made with this model, using the relation

$$\begin{aligned} [v_{g\perp}/Z(0)]_{\text{expt}} &= (\hbar k_{\perp} / m_0) / [Z(0)m_b/m_0] \\ &= (\hbar k_{\perp} / m_0) / Z^*(0), \end{aligned}$$

where $[v_{g\perp}/Z(0)]_{\text{expt}}$ are the experimental values measured here using Tomasch techniques, gave an average value of $Z^*(0) = 2.14$, very close to the value of just $Z(0)$ for polycrystal Pb. In other words, $Z^*(0)$ is increased by the ratio m_b/m_0 . The value $Z^*(0)$ on the average agrees, within experi-

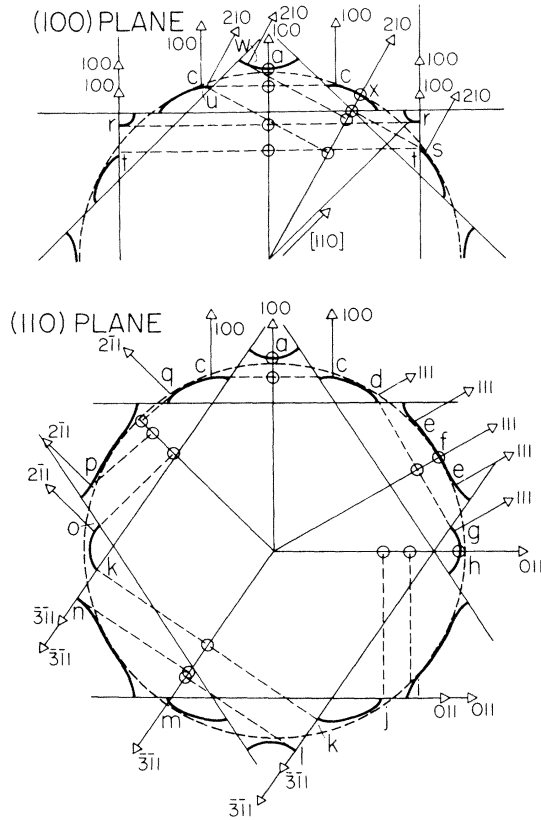


FIG. 4. Sections of the Fermi surface of Pb showing the sites which contribute to tunneling in each direction (arrows) and indicating the respective k_{\perp} involved in the Tomasch oscillations (small circles).

mental error, with the value of $Z(0)$ obtained by McMillan and Rowell. But this is really nothing more than using m_0 instead of m_b in the first place to calculate $v_{g\perp}$ from the data of Anderson and

Gold³ using the methods of Lykken *et al.*²

Unfortunately this comparison is not quite straightforward since a major difficulty in the study lay in associating each $[v_{g\perp}/Z(0)]_{\text{expt}}$ with a specific point on the Fermi surface. Some oscillations were not always present in the tunneling data. It was not possible or necessary, therefore, to have every point indicated in Fig. 4 represented in the data. Occasionally, however, Tomasch oscillations which were obviously not sinusoidal near the conductance peak nevertheless showed only a single peak in the Fourier spectrum. The behavior could only be interpreted as due to two oscillations of the same frequency; one from each of two gaps. The rapid change in relative amplitudes near the gap structure produced a distortion which was not present at higher voltages where the bulk of the Fourier integration occurred.

The values of $[v_{g\perp}/Z(0)]_{\text{expt}}$ were identified with a specific point on the Fermi surface by theoretically reconstructing the oscillations using the gap parameters to obtain a phase match between the calculated and experimental curves. It was found that associating an oscillation with one experimentally measured gap generally shifted its phase by about π from that associated with the other experimentally measured gap. In several instances the phase match was made using a gap intermediate in value between the two experimental gaps. In these cases the oscillation was assigned to both gaps and it was assumed that two oscillations with the same frequency were present. This technique and/or the one described in the previous paragraph had to be used wherever two or more values of $[v_{g\perp}/Z(0)]_{\text{expt}}$ appear the same for a given orientation in Tables II and III. No fit could be obtained for the [210] data by this method. For the [211] data only the high-velocity oscilla-

TABLE II. Fermi-surface parameters for the principal directions.

Tunneling direction	Zone	Point on Fermi surface	$(\hbar k_{\perp}/m_0)_{\text{theor}}$ (10^8 cm/sec)	$[v_{g\perp}/Z(0)]_{\text{expt}}^a$ (10^8 cm/sec)	$[Z^*(0)]_{\text{expt}}$	Δ_0 expt (meV)	Δ_0 theor (Ref. 9) (meV)
[100]	2	a	1.9	0.79	2.2	1.43	1.4
	2	r	1.54	0.64	2.4	1.20	...
	3	c	1.7	0.64	2.7	1.37	1.38
	3	t	1.3	0.64	2.0	1.20	...
[111]	2	e	1.85	0.94	2.0	1.20	1.36
	2	f	1.85	0.94	2.0	1.37	1.36
	3	d	1.63	0.65	2.5	1.37	1.35
	3	g	1.57	0.65	2.4	1.37	1.35
[110]	2	i	1.35	0.63	2.1	1.37	1.35
	3	h	1.73	0.85	2.0	1.24	1.27
	3	j	1.01	0.54	1.9	1.37	1.36

^a Specific zone assignments are tentative. See text for explanation.

TABLE III. Fermi-surface parameters for nonprincipal directions.

Tunneling direction	Zone	Point on Fermi surface	$(\hbar k_{\perp}/m_0)_{\text{theor}}$ (10^9 cm/sec)	$[v_{g\perp}/Z(0)]_{\text{expt}}^a$ (10^9 cm/sec)	$[Z^*(0)]_{\text{expt}}$	Δ_0 expt (meV)	Δ_0 theor (Ref. 9) (meV)
[211]	2	<i>p</i>	1.7	0.94	1.8	1.4	1.33
	3	<i>o</i>	1.31	0.67	1.9	...	1.28
	3	<i>q</i>	1.84	0.67	2.7	...	1.36
[311]	2	<i>l</i>	1.50	0.86	1.8	1.2	1.33
	2	<i>n</i>	1.50	0.86	1.8	1.2	1.33
	3	<i>k</i>	1.10	0.64	1.7	1.4	1.28
	3	<i>m</i>	1.84	0.64	2.9	1.4	1.37
[210]	2	<i>w</i>	1.56	0.80	2.0	...	1.35
	3	<i>x</i>	1.86
	3	<i>s</i>	1.68
	3	<i>u</i>	1.20	0.52	2.3

^aSpecific zone assignments are tentative. See text for explanation.

tion could be fitted as it dominated the smaller velocity in all samples.

The gap values thus obtained were compared with those calculated by Bennett¹⁰ in order to identify

them with a portion of the Fermi surface. In cases where this fit resulted in values of $Z^*(0)$ outside the range 2.3 ± 0.6 , sites were selected to bring the value of $Z^*(0)$ within this range. The results

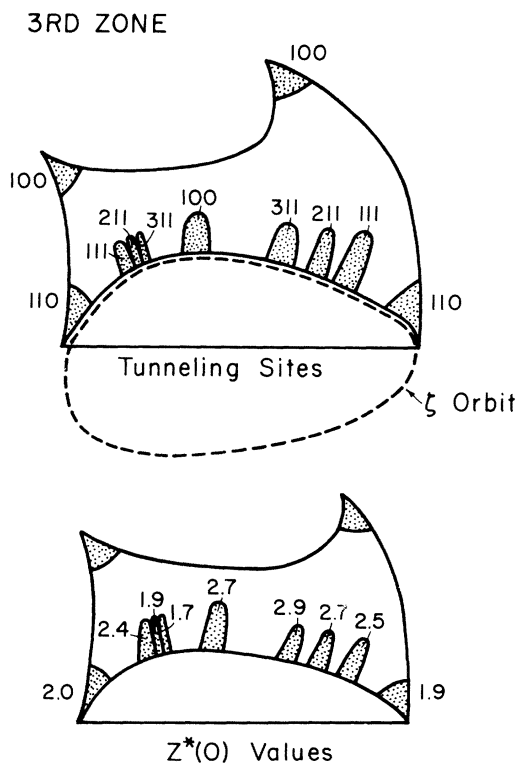


FIG. 5. Portion of the third zone of lead in the reduced zone scheme shown in perspective. The dashed line shows the de Haas-van Alphen ζ orbit as denoted by Anderson and Gold (Ref. 3). Shaded areas indicate approximate portions on the surface sampled by electrons tunneling in the directions indicated (tunneling sites). The $Z^*(0)$ value for each sampled portion is shown in the lower illustration. (Also see Fig. 7).

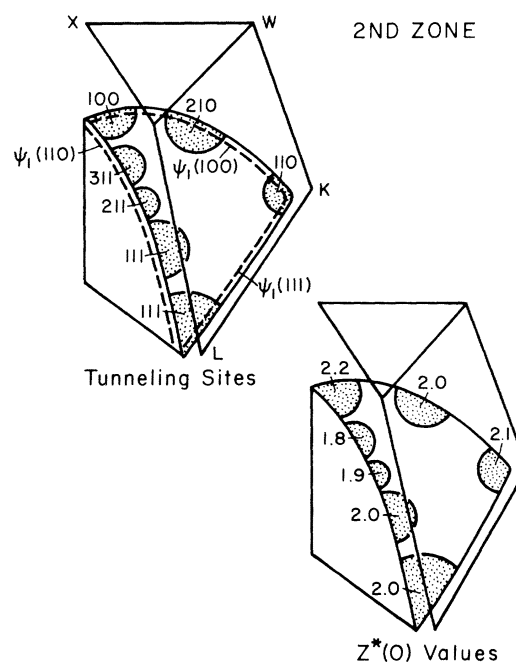


FIG. 6. Portion of the primitive Brillouin zone for the fcc structure enclosing the second-zone hole surface of lead in the reduced zone scheme. The lettered corners are standard crystallographic points on the Brillouin zone which define the portion illustrated. Dashed lines are de Haas-van Alphen orbits as denoted by Anderson and Gold (Ref. 3). Shaded areas indicate approximate portions on the surface sampled by electron tunneling in the directions indicated. The $Z^*(0)$ value for each sampled portion is shown in the lower illustration.



FIG. 7. Portion of the third-zone electron surface of lead showing the location of the section depicted in Fig. 3. Modified from, M. Ya. Azbel, M. I. Kaganov, and L. M. Lifshitz, *Conduction Electrons in Metals* (Freeman, San Francisco, 1973), Copyright © 1973 by Scientific American, Inc. All rights reserved.

of this fitting are summarized in Tables II and III.

The nature of the variation in $Z^*(0)$ over the Fermi surface is more easily seen in the reduced zone, shown in Figs. 5, 6, and 7. Most apparent is the systematic reduction of $Z^*(0)$ at the zone boundaries: the [110] and [311] directions in the third zone and the [311] direction in the second zone. It is also evident that the average value of $Z^*(0)$ in the second zone is lower than that of the third zone.

A calculation of $Z(0)$ was made by Anderson and Gold³ and later by Anderson, O'Sullivan, and Schirber¹³ (AOS) by comparing the ratio of the cyclotron-resonance effective mass to those calculated using the de Haas-van Alphen-based models of the Fermi surface for various orbits on the Fermi surface. As the effective mass as measured by cyclotron resonance includes the phonon renormalization and since the effective mass as calculated from a band structure fitted to de Haas-van Alphen data does not include the phonon renormalization,¹⁴ the ratio of these effective masses in just $Z(0)$ For the ζ orbit shown in Fig. 5 AOS

calculate $Z(0)=2.5$. The average value of $Z^*(0)$ from this experiment for that orbit is 2.3, giving each value the same weight in the average. As the low values of $Z^*(0)$ are found at zone boundaries, one might assume that the greater part of the Fermi surface over the ζ orbit would reflect a larger value than this average. For the $\psi_1(110)$ orbit of Fig. 6 AOS calculate $Z(0)\approx 2.0$. The average of that orbit for $Z^*(0)$ in this experiment is also 2.0. This agreement between $Z(0)$ and $Z^*(0)$ implies that $m_b/m_0\approx 1$ over the Fermi surface of superconducting Pb for the quasiparticles involved in the Tomasch effect. This result may imply that the electron-pairing interaction in superconducting Pb dominates the electron-ion interaction to the extent that band effects are negligible in the effective mass. However, it should be noted that the fitting procedures previously described are somewhat speculative and that only the average value of $Z^*(0)$ contains no ambiguity.

V. SUMMARY

This study has developed a new analysis technique for Tomasch oscillation periods. With this technique values of $v_F/Z(0)$ for single-crystal Pb films have been found to differ in some cases from those previously reported both in value and in the number of discrete velocities present for a given tunneling direction. The new technique has, for the first time, resolved in Tomasch oscillations structure which can be interpreted as harmonic in nature. An attempt based on the group-velocity tunneling selection rule has been made to identify the various oscillations with distinct portions of the Fermi surface. The results of this fitting show that the effective mass of electrons with phonon renormalization, $Z^*(0)=Z(0)m_b/m_0$, is uniformly lower for electrons in the second zone than for those in the third zone, and that values of $Z^*(0)$ at zone boundaries is lower than the surrounding areas on the Fermi surface. The values obtained for $Z^*(0)$ agree qualitatively with those of $Z(0)$ calculated by Anderson, O'Sullivan, and Schirber¹³ and imply that the effective band mass m_b of superconducting quasiparticles in Pb is approximately equal to the free-electron mass.

The authors would like to acknowledge Dr. K. S. Dy and Dr. J. W. Baker for many helpful discussions.

*This work was supported in part by the Materials Research Center, U.N.C. under Grant No. GH-33632 from the National Science Foundation.

†Present address: Department of Materials Science

and Engineering, Cornell University, Ithaca, N. Y. 14850.

‡Present address: Republic Steel Corp., Research Center, Independence, Ohio 44131.

- ¹W. J. Tomasch, Phys. Rev. Lett. 15, 672 (1965).
²G. I. Lykken, A. L. Geiger, K. S. Dy, and E. N. Mitchell, Phys. Rev. B 4, 1523 (1971).
³J. R. Anderson and A. V. Gold, Phys. Rev. 150, 356 (1966).
⁴W. L. McMillan and J. M. Rowell, Phys. Rev. Lett. 14, 108 (1965).
⁵T. W. Haywood, thesis (University of North Carolina, 1974) (unpublished).
⁶D. J. Scalapino, in *Superconductivity*, edited by R. D. Parks (Marcel Dekker, New York, 1969), Vol. 1, p. 533.
⁷T. Wolfram, Phys. Rev. 170, 481 (1968).
⁸J. E. Dowman, M. L. A. MacVicar, and J. R. Waldram, Phys. Rev. 186, 452 (1969).
⁹T. W. Haywood and E. N. Mitchell, Phys. Rev. B 10, 876 (1974).
¹⁰A. J. Bennett, Phys. Rev. 140, A1902 (1965).
¹¹B. L. Blackford, Physica (Utr.) 55, 475 (1971).
¹²W. L. McMillan and P. W. Anderson, Phys. Rev. Lett. 16, 85 (1966).
¹³J. R. Anderson, W. J. O'Sullivan, and J. E. Schirber, Phys. Rev. B 5, 4683 (1972).
¹⁴R. E. Prange and L. P. Kadanoff, Phys. Rev. 134, A566 (1964).

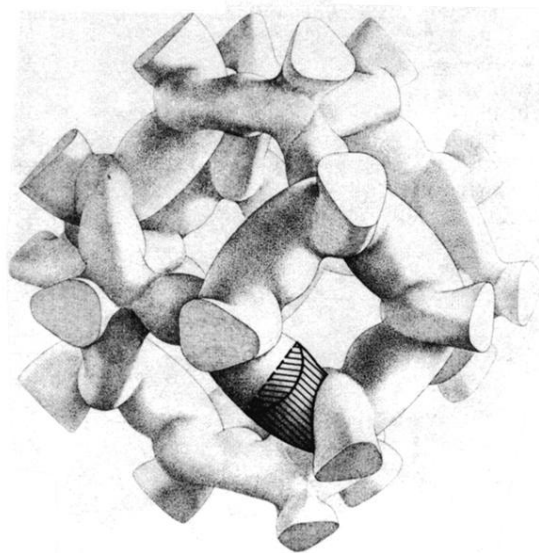


FIG. 7. Portion of the third-zone electron surface of lead showing the location of the section depicted in Fig. 3. Modified from, M. Ya. Azbel, M. I. Kaganov, and L. M. Lifshitz, *Conduction Electrons in Metals* (Freeman, San Francisco, 1973), Copyright © 1973 by Scientific American, Inc. All rights reserved.